






## Ultrafast nuclear dynamics in double-core-ionized water molecules

Iyas Ismail <sup>1,\*</sup>,<sup>†</sup> Ludger Inhester <sup>2,\*</sup>,<sup>‡</sup> Tatiana Marchenko <sup>1</sup>, Florian Trinter,<sup>3,4</sup> Abhishek Verma,<sup>1</sup> Alberto De Fanis,<sup>5</sup> Anthony Ferté,<sup>1</sup> Daniel E. Rivas,<sup>5</sup> Dawei Peng,<sup>1,5</sup> Dimitris Koulentianos,<sup>6</sup> Edwin Kukk,<sup>1,7</sup> Francis Penent,<sup>1</sup> Gilles Doumy,<sup>6</sup> Giuseppe Sansone,<sup>8</sup> John D. Bozek,<sup>9</sup> Kai Li,<sup>6,10</sup> Linda Young,<sup>6,10</sup> Markus Ilchen,<sup>5</sup> Maria Novella Piancastelli,<sup>1</sup> Michael Meyer,<sup>5</sup> Nicolas Velasquez,<sup>1</sup> Oksana Travnikova <sup>1</sup>, Rebecca Boll <sup>5</sup>, Renaud Guillemin,<sup>1</sup> Reinhard Dörner,<sup>3</sup> Richard Taïeb,<sup>1</sup> Simon Dold,<sup>5</sup> Stéphane Carniato,<sup>1</sup> Thomas M. Baumann,<sup>5</sup> Tommaso Mazza,<sup>5</sup> Yevheniy Ovcharenko,<sup>5</sup> Ralph Püttner,<sup>11</sup> and Marc Simon<sup>1</sup>

<sup>1</sup>*Sorbonne Université, CNRS, Laboratoire de Chimie Physique-Matière et Rayonnement, LCPMR, 75005 Paris Cedex 05, France*

<sup>2</sup>*Center for Free-Electron Laser Science CFEL, Deutsches Elektronen-Synchrotron DESY, Notkestraße 85, 22607 Hamburg, Germany*

<sup>3</sup>*Institut für Kernphysik, Goethe-Universität Frankfurt, Max-von-Laue-Straße 1, 60438 Frankfurt am Main, Germany*

<sup>4</sup>*Molecular Physics, Fritz-Haber-Institut der Max-Planck-Gesellschaft, Faradayweg 4-6, 14195 Berlin, Germany*

<sup>5</sup>*European XFEL, Holzkoppel 4, 22869 Schenefeld, Germany*

<sup>6</sup>*Chemical Sciences and Engineering Division, Argonne National Laboratory, 9700 South Cass Avenue, Lemont, Illinois 60439, USA*

<sup>7</sup>*Department of Physics and Astronomy, University of Turku, 20014 Turku, Finland*

<sup>8</sup>*Institute of Physics, University of Freiburg, Hermann-Herder-Straße 3, 79104 Freiburg, Germany*

<sup>9</sup>*Synchrotron SOLEIL, L'Orme des Merisiers, Saint-Aubin, 91192 Gif-sur-Yvette Cedex, France*

<sup>10</sup>*Department of Physics and James Franck Institute, The University of Chicago, Chicago, Illinois 60637, USA*

<sup>11</sup>*Fachbereich Physik, Freie Universität Berlin, Arnimallee 14 14195 Berlin, Germany*



(Received 12 March 2024; revised 31 May 2024; accepted 13 June 2024; published 10 July 2024)

Double-core-hole (DCH) states in isolated-water and heavy-water molecules, resulting from the sequential absorption of two x-ray photons, have been investigated. A comparison of the subsequent Auger emission spectra from the two isotopes provides direct evidence of ultrafast nuclear motion during the 1.5-fs lifetime of these DCH states. Our numerical results align well with the experimental data, providing for various DCH states an in-depth study of the dynamics responsible of the observed isotope effect.

DOI: [10.1103/PhysRevA.110.013108](https://doi.org/10.1103/PhysRevA.110.013108)

### I. INTRODUCTION

Double-core-hole (DCH) states refer to electronic states with two vacancies in the core level. Spectroscopy of DCH states stands out as a highly promising tool, showing a remarkably enhanced sensitivity to the chemical environment when compared to single-core-hole (SCH) spectroscopy [1–8]. Moreover, specifically for double vacancies in the  $K$  shell, the significantly lower lifetime of these states, compared to SCH states [9–11], positions this emerging spectroscopy as a powerful femtosecond probe, enabling the tracking of nuclear dynamics occurring during the first (sub)femtoseconds of the interaction with the light.

Core-hole and double-core-hole states have received considerable attention due to the fact that these hollow electronic configurations have a temporarily reduced x-ray absorption cross section, leading to an effect termed “x-ray-induced transparency” or “frustrated absorption” [12,13]. This becomes relevant for prospective single-molecule diffractive imaging, where radiation damage can potentially be suppressed through sufficiently short x-ray pulses [5,14].

Double vacancies in the core level were first observed in nuclear reactions [15,16], as well as collisions involving mul-

ticharged ions [17] and electrons [18]. Substantial progress has been made through the utilization of synchrotron light sources, enabling the production of DCH states through one-photon absorption (see, e.g., Refs. [11,19–24]). In this case, DCH states appear as satellites of the one-photon core ionization and are referred to as hypersatellites [16]. Furthermore, the use of highly intense light sources such as x-ray free-electron laser (XFEL) facilities, enables the creation of DCH states through sequential two-photon absorption (see, e.g., Refs. [3,4,12,25–27]). For that purpose, the absorption of the second photon has to occur before the decay of the SCH state. Previous studies have explored a large variety of such states. Specifically, for vacancies in the  $K$  shell, states were investigated in which either both core-level electrons were ejected to the continuum ( $K^{-2}$  state) or one electron was ejected to the continuum while the other one was excited to a vacant orbital  $V$  ( $K^{-2}V$  states) or both core-level electrons were excited to vacant orbitals ( $K^{-2}VV'$  states). For low- $Z$  elements,  $K$ -shell holes decay predominantly nonradiatively via Auger decay. In this process, an electron from a valence level fills one of the core holes, while another electron is emitted to the continuum. For DCH states in the  $K$  shell, this Auger electron has significantly higher kinetic energy compared to the Auger electron created from SCH states. This difference in kinetic energy allows for the separation of the signal originating from DCH states from the signal of the SCH states. The emitted Auger electron is thereby a clear probe of DCH states.

\*These authors contributed equally to this work.

<sup>†</sup>Contact author: [iyas.ismail@sorbonne-universite.fr](mailto:iyas.ismail@sorbonne-universite.fr)

<sup>‡</sup>Contact author: [ludger.inhester@cfel.de](mailto:ludger.inhester@cfel.de)

In order to characterize the dynamics of DCH states, which is potentially relevant for x-ray diffractive imaging, and to exploit the chemical sensitivity of their spectroscopic signals, it is crucial to understand the electronic spectra of DCH states. Earlier studies demonstrated the presence of strongly dissociative potential-energy surfaces (PESs) in DCH states of HCl and CH<sub>3</sub>I molecules [28,29]. For water, a theoretical study by Inhester *et al.* [30] showed that the produced Auger spectrum is considerably influenced by the involved steep PES. This prediction was corroborated by a recent study [11] conducted by some of the present authors which revealed an indication of ultrafast proton motion within the very short lifetime (about 1.5 fs [30]) of the DCH states in water molecules, leaving significant fingerprints in the Auger emission spectrum. Furthermore, within the same study, theoretical predictions indicated significant variations in the dynamic response depending on the specific populated DCH states, namely,  $K^{-2}$  or  $K^{-2}V$ . Notably, some  $K^{-2}V$  states turned out to be more dissociative than the bare  $K^{-2}$  state.

This theoretical finding could not be directly confirmed through experimental observation because the photon intensity provided by the synchrotron radiation source allowed the simultaneous population of multiple DCH states via only one-photon shake-up and shake-off processes. Consequently, only an overall Auger spectrum containing contributions from several DCH ( $K^{-2}$ ,  $K^{-2}V$ ) states could be measured.

In this paper, we present a more direct measurement of the Auger emission from DCH states using an XFEL light source combined with a comprehensive theoretical investigation of the ultrafast motion following the generation of *specific* DCH states in water molecules. In particular, by employing x-ray light of sufficient intensity, we study DCH states produced via sequential absorption of two photons. By tuning the employed photon energy, we explore the spectrum variations of the emitted Auger electron when addressing regimes leading predominantly to  $K^{-2}$  states via sequential core-shell photoionization or to  $K^{-2}V$  states via subsequent core-shell photoionization and core-shell photoexcitation. This enables distinct investigations of the subsequent dynamics associated with each of these states. Moreover, by comparing Auger spectra obtained from isolated-water (H<sub>2</sub>O) and heavy-water (D<sub>2</sub>O) molecules, we provide unequivocal evidence of ultrafast dynamics occurring during the 1.5-fs lifetime of the DCH state.

The outline of this paper is as follows: Sec. II describes the experimental setup; Sec. III describes the calculation methodology. The resulting measured and calculated Auger spectra are discussed in Sec. IV, and in Sec. V, we draw final conclusions.

## II. EXPERIMENT

The experiment was conducted using the atomiclike quantum system (AQS) end station at the Small Quantum Systems (SQS) instrument located at the SASE3 undulator of the European XFEL [31–33]. The XFEL beam, with a pulse energy of approximately 4 mJ, delivered 30 pulses per train at a repetition rate of 1.1 MHz within the train, while the trains operated at a repetition rate of 10 Hz. The XFEL beam pulses, with a duration of about 25 fs and a bandwidth of roughly 6

to 7 eV for photon energies in the range from 600 to 750 eV, were focused to approximately  $1.5 \times 1.5 \mu\text{m}^2$ .

With the given pulse parameters and considering a Gaussian temporal pulse shape and a rate-equation model, we estimate the ratio for sequential core-shell ionization processes vs core-shell ionization followed by Auger decay (DCH-to-SCH ratio) as 0.86. We note, however, that this is an upper estimate of this ratio since many molecules are not ionized in the center of the x-ray pulse.

Electrons were detected with a time-of-flight (TOF) spectrometer installed facing the AQS chamber ionization region, where the x-ray focus was optimized. The spectrometer was oriented at the magic angle ( $54.7^\circ$ ) with respect to the horizontal linear polarization of the photon beam. A retardation potential of 500 V was applied to improve the energy resolution of the spectrometer for the measured Auger electrons. The energy resolution was about 900 meV for kinetic energy around 550 eV. The electrons were detected using commercially available microchannel-plate detectors. More details about the TOF spectrometer can be found elsewhere [34]. Water molecules H<sub>2</sub>O and D<sub>2</sub>O were introduced using a bubbler system connected to the ultrahigh-vacuum interaction chamber, resulting in a pressure of about  $4.6 \times 10^{-8}$  mbar in the experimental chamber under gas load. The TOF spectrometer was energy calibrated using the H<sub>2</sub>O outer-valence photoelectron lines. The photon energy was calibrated with the  $K^{-2}$  states of water [11]. Additionally, the TOF transmission curves were derived by normalizing the yield of the H<sub>2</sub>O photoelectron lines.

## III. THEORETICAL CALCULATIONS

In order to calculate the DCH-Auger spectra of water, we employed the XMOLECULE electronic-structure tool kit (version 3869) [35,36]. Specifically, we computed double-core-ionized states ( $K^{-2}$  and various  $K^{-2}V$  configurations) using the restricted Hartree-Fock method. Convergence to the desired states was achieved based on the maximum-overlap method [37,38]. All calculations were performed using the augmented correlation-consistent polarized valence triple zeta (aug-cc-pVTZ) basis set [39,40]. With the orbitals optimized for the initial double-core-ionized state, we compute the final electronic states using configuration interaction. All direct final Auger configurations (one core hole and two valence holes) as well as configurations with additional excitation into previously unoccupied (virtual) orbitals (one core hole, three valence holes, and one virtual electron) were taken into account for the configurational expansion of the final states. Note that the latter configurations can also describe shake processes during the Auger decay.

The Auger amplitudes were calculated using the one-center approximation [41] that treats the Auger process as a largely intra-atomic transition and approximates the molecular continuum wave functions with the corresponding atomic continuum wave functions. In XMOLECULE, atomic continuum matrix elements from atomic calculations using XATOM [42] are used.

The effects of nuclear dynamics in the spectrum were incorporated following Refs. [11,30]. A set of 100 molecular dynamics (MD) trajectories was propagated on the respective

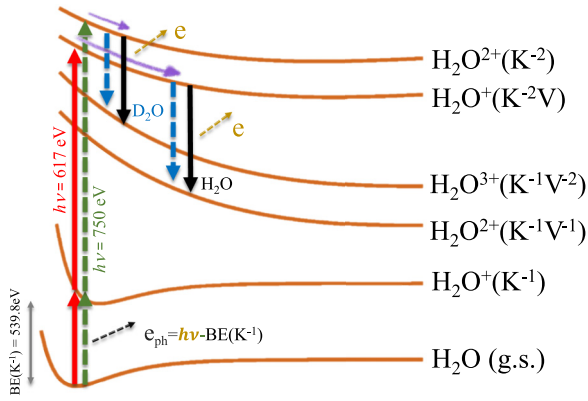


FIG. 1. Schematic illustration of the potential-energy surfaces of  $K^{-2}$  and  $K^{-2V}$  along the dissociation coordinate. Using two photons of 750-eV energy, the  $K^{-2}$  state is produced through sequential ionization:  $\text{H}_2\text{O}$  (g.s.)  $\rightarrow$   $\text{H}_2\text{O}^+$  ( $K^{-1}$ )  $\rightarrow$   $\text{H}_2\text{O}^{2+}$  ( $K^{-2}$ ). Nuclear motion occurs along the dissociative  $K^{-2}$  potential-energy surface. Over the 1.5-fs lifetime, the protons explore a greater distance along the dissociation coordinate than the deuterons, leading to noticeable differences in the Auger-electron energy, which are larger for water (black arrow) than for heavy water (blue arrow). With photons of 617-eV energy, the  $K^{-2V}$  state is populated via the following excitation scheme:  $\text{H}_2\text{O}$  (g.s.)  $\rightarrow$   $\text{H}_2\text{O}^+$  ( $K^{-1}$ )  $\rightarrow$   $\text{H}_2\text{O}^+$  ( $K^{-2V}$ ). In this case, a nuclear motion similar to that of the  $K^{-2}$  state arises.

double-core-ionized state with a time step of 0.1 fs for a total time of 20 fs. These trajectories started from initial conditions sampled from the neutral ground-state Wigner distribution. For each time step of the MD trajectories, instantaneous Auger spectra  $T(E, t)$  were calculated, where for each transition a Lorentzian line shape was employed. The total Auger spectrum was then compiled using [11]

$$T(E) = \int dt T(E, t) e^{-\Gamma t}, \quad (1)$$

where  $\Gamma$  is the calculated reciprocal lifetime of the double-core-hole configuration. For the final spectrum, we also take into account a further convolution with a Gaussian function with a full width at half maximum of 900 meV to account for the finite resolution in the experiment. For a better comparison with the experiment, the calculated Auger spectra were further shifted by 5 eV to lower energies. This shift compensates for an imbalance between the initial and final electronic states that occurs due to the orbital optimization for the initial electronic state and the inclusion of several valence-to-virtual excitations for the final electronic states. In addition, it compensates for relativistic effects in the oxygen core level that are not considered in the calculation. See Appendix B for further discussion of the shift.

#### IV. RESULTS AND DISCUSSION

Figure 1 sketches the PESs that are populated in the experiment via subsequent core-ionization and core-excitation steps. Whereas there is little dynamics involved in the first core-ionization step [30], the second core-ionization or core-excitation step induces ultrafast dissociation of the molecule. The emission of an Auger electron brings the molecule en-

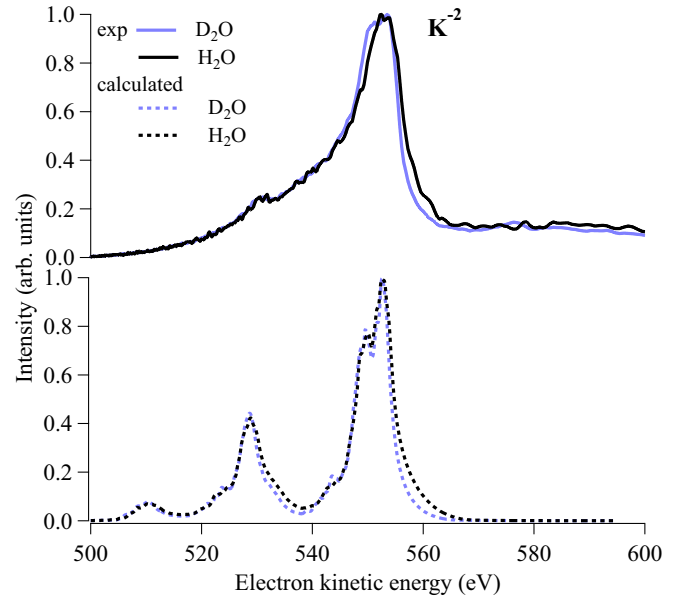


FIG. 2. Comparison of experimental Auger spectra measured with a photon energy of 750 eV (solid lines) with calculated Auger spectra for the  $K^{-2}$  state (dashed lines). Black lines show spectra for water; blue lines show spectra for heavy water. The spectra are normalized to have similar peak heights.

ergetically down either to the dicationic or tricationic state. Because these states involve a larger charge in the molecule, the PESs along the dissociation coordinate become, in general, steeper. Because of this differential gradient of the PESs along the dissociation coordinate, the emission energy of the Auger electron shifts to higher energies the further the dissociative dynamics in the DCH state proceeds. We note that the scheme presented in Fig. 1 allows us to map out dynamics on a timescale much faster than the pulse duration, which is about 25 fs for the current experiment. This is enabled by focusing on features specifically related to DCH states, which have a very short lifetime, and the fact that no essential dynamics occurs on the preceding SCH state [30].

The experimental Auger spectra, measured at a photon energy of 750 eV for both water and heavy water, are shown in Fig. 2 along with the calculated spectra for comparison. At this photon energy, the x-ray pulse can core ionize the water molecule in sequential steps, producing mostly the bare  $K^{-2}$  state. The difference between water and heavy water can be seen mainly at 560 eV, on the high-energy side of the dominant Auger peak. One can see that the tail to higher energies is much more pronounced for water than for heavy water. This trend is in good agreement with the calculated Auger spectra.

Overall, the calculation reproduces all the characteristic features of the experimental Auger spectrum. However, in the experimental spectra additional contributions appear in the range 530–540 eV. We attribute this discrepancy to  $K^{-2V^{-1}}$  configurations, as discussed in Appendix A.

In Fig. 3, we show the Auger spectra measured at a photon energy of 617 eV. At this photon energy, DCH states are created by a sequence of core-ionization and resonant core-excitation steps, producing singly charged  $K^{-2V}$  configurations, as discussed in Fig. 1. The Auger features between

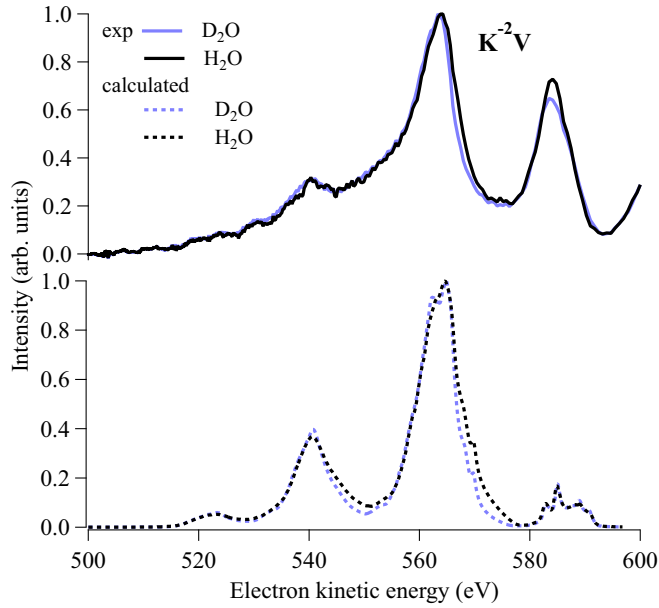


FIG. 3. Comparison of experimental spectra measured with a photon energy of 617 eV (solid lines) with calculated Auger spectra for a mixture of  $K^{-2}V$  states (dashed lines). Black lines show spectra for water; blue lines show spectra for heavy water. The spectra are normalized to have equal maximum peak heights. The experimental spectra show valence photoelectron lines overlapping with the participator Auger contribution located around 585 eV.

515 and 575 eV appear qualitatively similar to those measured at a photon energy of 750 eV (Fig. 2) but are shifted to higher kinetic energies. The feature observed at 585 eV can be partially attributed to participator Auger transitions involving the additional electron present in the  $V$  orbital. Because of the resonance condition, direct valence photoionization appears at the same photoelectron energy as the participator Auger energies. In Fig. 3, the participator transitions thus overlap with the photoelectron signal from valence ionization of  $H_2O^+$  ( $K^{-1}$ ), as shown in Ref. [27]. Because the employed photon bandwidth is rather broad, it fully covers the participator-Auger contribution above 585 eV. Notably, the valence-photoelectron signal is not considered in the theoretical calculations, which explains the difference between the calculated and observed intensities for this spectral feature.

The experimental spectrum shows a significant difference between water and heavy water in the main Auger peak at 565 eV following the same trend as previously observed in Fig. 2.

The broad photon bandwidth leads to the formation of a mixture of several  $K^{-2}V$  states. For the comparison with calculation results, the corresponding calculated Auger spectra are compiled from a mixture that is determined using the configuration-interaction calculations outlined in Ref. [27]. These calculations lead us to the following compositions of  $K^{-2}V$  states:  $0.24(K^{-2}4a_1) + 0.52(K^{-2}2b_2) + 0.16(K^{-2}2b_1) + 0.08(K^{-2}5a_1)$ . Using this mixture, the computed Auger spectra show a similarity to the experimental spectra as in Fig. 2. Specifically, the trend showing a more pronounced tail for water than for heavy water is reproduced. Like in Fig. 2, the lower-energy parts of the Auger spectra

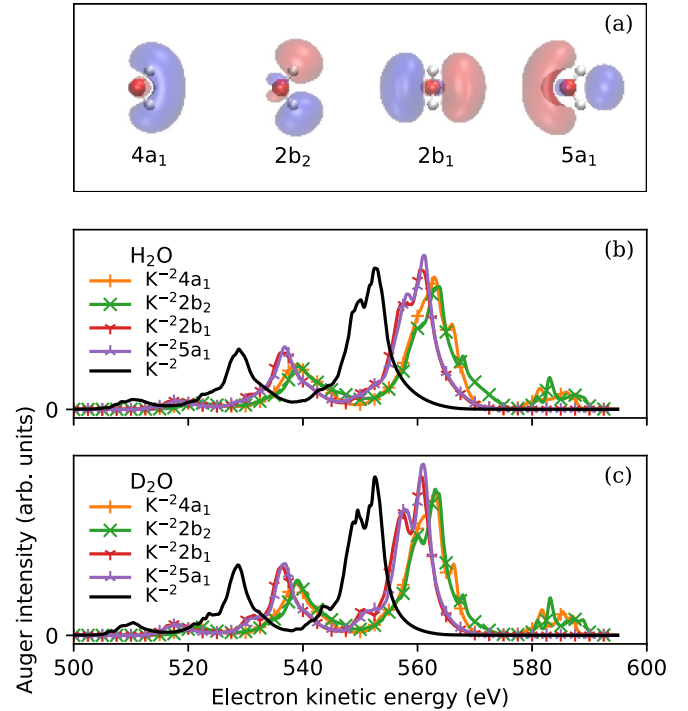


FIG. 4. (a) Isosurface plots for the virtual orbitals of the  $K^{-2}$  dication. Calculated Auger spectra for individual  $K^{-2}$  and  $K^{-2}V$  DCH states of (b)  $H_2O$  and (c)  $D_2O$ .

are considerably sharper in the calculated spectra compared with the measured spectra. We attribute these discrepancies to additional valence-ionization and valence-excitation processes due to shake processes and direct valence ionization (see Appendix A).

The clear isotope effect and the good agreement with the calculated spectra in Figs. 2 and 3 unequivocally establish the pronounced effects induced by the rapid proton dynamics of the Auger spectra, confirming previous findings [11].

Figure 4 displays the calculated Auger spectra for the  $K^{-2}$  state and the individual  $K^{-2}V$  states. Figure 4(a) shows an isosurface plot of the respective virtual orbitals of the  $K^{-2}$  dication that are populated in the respective  $K^{-2}V$  states. The spectra highlight the individual contributions of the resonances to shaping the high-energy tail of the main peak. As one can see, a participator contribution above 580 eV appears for the  $K^{-2}4a_1$  and the  $K^{-2}2b_2$  configurations. For the more highly excited  $K^{-2}2b_1$  and  $K^{-2}5a_1$  configurations they are practically absent because of the diffuse character of the orbitals, leading to very small Auger amplitudes for the involved transitions. The Auger spectra of these two higher-excitation DCH states are very similar to that of the  $K^{-2}$  configuration but are shifted by about 7 eV to higher energies, indicating that the impact of having an additional electron in the  $5a_1$  or the  $2b_1$  orbital essentially amounts to screening of the ion charge.

The computational results allow us to inspect the dynamics in the  $K^{-2}$  state and various  $K^{-2}V$  states that are responsible for the isotope effect in more detail.

Figure 5 shows calculated spectra from the ensemble of trajectories after selected times of dynamics for the ensemble of  $K^{-2}V$  states considered in Fig. 3. Spectra for  $H_2O$



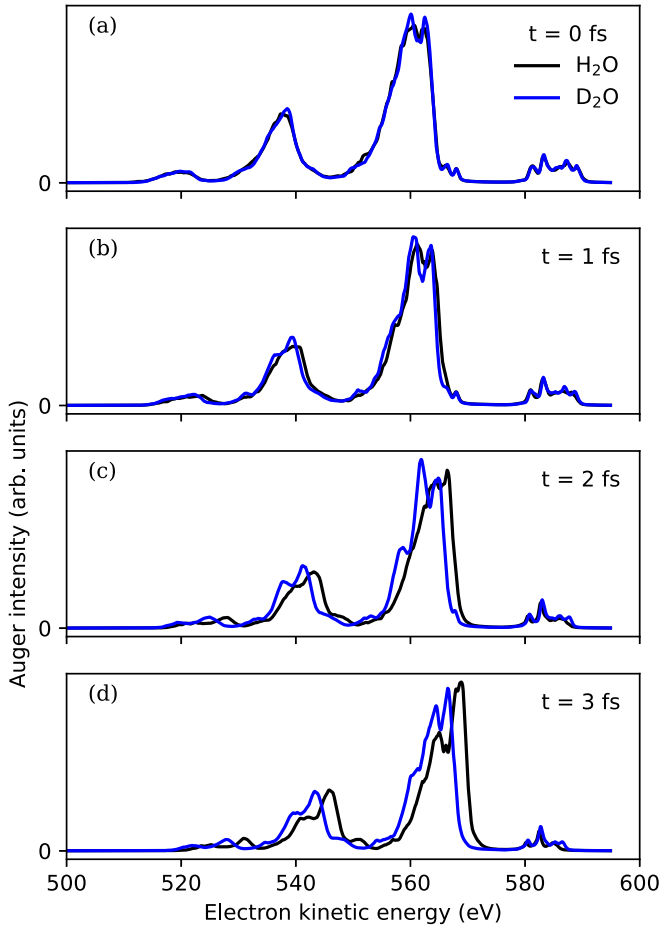


FIG. 5. Calculated instantaneous Auger spectra for selected times after core ionization for an ensemble of  $K^{-2}V$  states for  $H_2O$  (black line) and  $D_2O$  (blue line).

as well as for  $D_2O$  are shown. These instantaneous spectra nicely illustrate how the resulting spectra display effects of core-hole-state dynamics emerging in the marked tail on the high-energy side of the dominant Auger peak.

As time progresses [Figs. 5(b)–5(d)], the Auger spectrum gradually shifts to higher energies. This shift is stronger for  $H_2O$  and can be qualitatively understood from the fact that the emission of protons or deuterons transports charge away from the oxygen atom. At later times, valence electrons thus experience lower Coulomb attraction, which in turn gives rise to faster Auger electrons. Remarkably, this shift does not occur for participator contributions above 580 eV, an observation that can be understood from the specific shape of the participator orbitals, as discussed later.

Even though the dynamics can be, overall, characterized by a rapid symmetric explosion of the molecule, the individual satellite states can have a pronounced characteristic core-hole-state dynamics [11].

Figure 6 shows how the asymmetry, the average OH (OD) bond distance, and the bond angle  $\alpha$  evolve as a function of time. To highlight these differences, the plots show the evolution of trajectories for up to 5 fs, even though one must keep in mind that the considered double-core-hole configurations have a lifetime of only about 1.5 fs, and it is thus, according

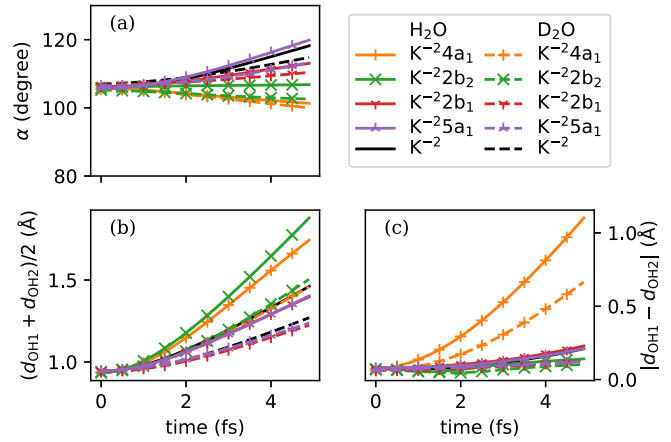


FIG. 6. Evolution of the internal coordinates (averaged over all trajectories) for individual double-core-hole states. (a) HOH and DOD bond angles. (b) Average oxygen-hydrogen and oxygen-deuterium distances. (c) Absolute difference in oxygen-hydrogen and oxygen-deuterium distances.

to the exponential-decay law, unlikely that such an electronic configuration is present for such a long time. As one can see, the  $K^{-2}$  configuration involves a largely symmetric dissociation into a doubly core-excited oxygen and two protons. The  $K^{-2}4a_1$  configuration shows a very strong asymmetric fragmentation [Fig. 6(c)]. In particular, the simulations reveal that this configuration asymptotically involves fragmentation into a  $K^{-2}V$  hydroxyl cation ( $OH^+$ ) and a proton. Such a strong antisymmetric character was also reported for the single-core-excited  $K^{-1}4a_1$  state [43]. Moreover, the  $K^{-2}$  and  $K^{-2}5a_1$  configurations show a trend for HOH angle-opening dynamics, whereas the opposite (angle closing) can be seen for the  $K^{-2}4a_1$  configuration [Fig. 6(a)]. The configuration  $K^{-2}2b_2$  stands out because it exhibits a particularly rapid symmetric fragmentation [Fig. 6(b)]. Overall, one can see that the configurations  $K^{-2}4a_1$  and  $K^{-2}2b_2$  induce a somewhat more rapid fragmentation than the bare  $K^{-2}$  configuration, whereas more highly excited states like  $K^{-2}2b_1$  and  $K^{-2}5a_1$  show a fragmentation dynamics similar to the  $K^{-2}$  configuration. The variations between the  $K^{-2}V$  states can be understood from the influence of the electron in the previously unoccupied orbital [see Fig. 4(a)]. The antibonding character of the  $4a_1$  and the  $2b_2$  orbitals pushes the protons away more rapidly. In addition, the  $4a_1$  orbital has a bonding character between the hydrogen atoms and thus induces lowering of the HOH angle.

The antibonding character of the  $4a_1$  and  $2b_2$  orbitals also explains the distinct behavior of the participator lines along the dynamics observed in Fig. 5. Whereas the kinetic energy of the spectator-Auger electrons increases as the dissociation proceeds because the involved valence orbitals become less bound as the Coulomb attraction to the protons decreases with increased OH bond length, the participator contributions are also impacted by the respective orbital's antibonding character along the OH bond, making them *more strongly* bound as the dissociation proceeds. As a result, participator contributions do not shift that strongly in the instantaneous Auger spectra shown in Fig. 5.

## V. CONCLUSIONS

We experimentally and theoretically investigated double-core-hole states in isolated-water and heavy-water molecules generated through the sequential absorption of two x-ray photons. Theoretical calculations of the Auger process and the involved core-hole-state dynamics successfully reproduced the most distinct features of the experimental data, enabling an in-depth examination of the dynamics in  $K^{-2}$  and  $K^{-2}V$  states responsible for the observed isotope effect. Moreover, in the lower-energy part of the experimental DCH-Auger spectra, we identified additional Auger contributions that appear due to shake transitions in the two photoabsorption steps. Our measurements confirm earlier synchrotron measurements in which DCH states were created via one-photon absorption [11]. We note that analogous observations were very recently also made for the one-photon DCH-Auger spectrum of liquid water [44], demonstrating a considerable impact of the liquid environment on the DCH-Auger electron energy. The comparison of the Auger spectra obtained from the two isotopic systems in the gas phase provides an unequivocal confirmation of the ultrafast proton motion during the lifetime of the DCH states. By selectively populating different  $K^{-2}$  and  $K^{-2}V$  states, Auger spectra of both species could be disentangled, and distinct dynamic behaviors were observed. Further studies could consider investigating the ultrafast dynamics induced in DCH states by employing coincidence detection of ion fragments and electrons, which is feasible at the SQS instrument at European XFEL.

The experimental data were collected during user beam time 2620. The metadata are available from European XFEL [45].

## ACKNOWLEDGMENTS

We acknowledge European XFEL in Schenefeld, Germany, for the provision of XFEL beam time at the SQS instrument and thank the staff for their assistance. L.I. acknowledges support from DESY (Hamburg, Germany), a member of the Helmholtz Association HGF, and the scientific exchange and support of the Centre for Molecular Water Science (CMWS). A.F., R.T., and S.C. thank Labex MiChem, part of French state funds and managed by the ANR within the Investissements d'Avenir program (Sorbonne Université, ANR-11-IDEX-0004-02), for providing A.F.'s Ph.D. funding. D.P., A.V., J.D.B., and M.S. acknowledge the financial support of the CNRS and the GotoXFEL program. T. Marchenko and N.V. acknowledge funding from the European Union's Horizon 2020 research and innovation program under Marie Skłodowska-Curie Grant Agreement No. 860553. F.T. acknowledges funding from the Deutsche Forschungsgemeinschaft (DFG, German Research Foundation), Project No. 509471550, Emmy Noether Programme and acknowledges support from the MaxWater initiative of the Max-Planck-Gesellschaft. Work by D.K., K.L., G.D., and L.Y. was supported by the U.S. Department of Energy, Office of Science, Basic Energy Science, Chemical Sciences, Geosciences and Biosciences Division under Contract No. DE-AC02-06CH11357. M.M. acknowledges support from the DFG, German Research Foundation, SFB-925, Project No.

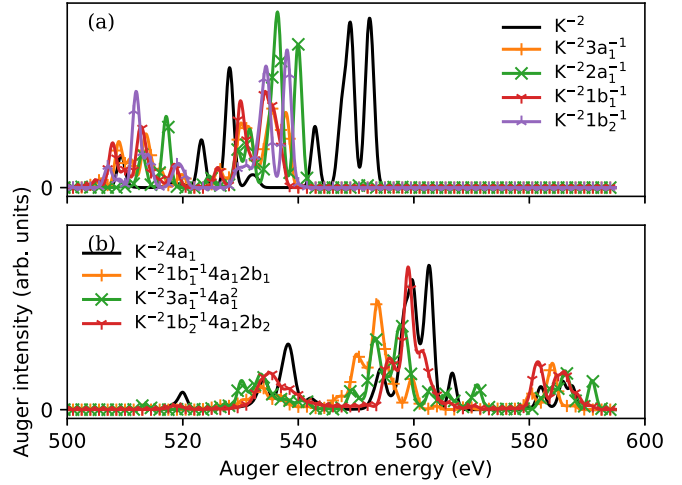


FIG. 7. Calculated DCH-Auger spectra for (a) additionally valence-ionized configurations and (b) additionally valence-excited configurations (equilibrium geometry only). The solid line shows results for the main  $K^{-2}(a)$  and  $K^{-2}4a_1$  configuration; the colored lines marked with crosses show results for various  $K^{-2}V^{-1}(a)$  and  $K^{-2}V^{-1}V'V''$  configurations.

170620586 and from the Cluster of Excellence Advanced Imaging of Matter of the DFG, EXC 2056, Project ID No. 390715994.

M.S., M.N.P., T. Marchenko, O.T., and I.I. conceptualized the work. I.I., T. Marchenko, F.T., A.V., A.D.F., D.E.R., D.P., D.K., E.K., F.P., G.D., G.S., J.D.B., K.L., L.Y., M.I., M.N.P., M.M., N.V., O.T., R.B., R.G., R.D., S.D., T.M.B., T. Mazza, Y.O., R.P., and M.S. conducted the experiments. I.I. and M.S. performed formal analysis. A.F., R.T., and S.C. provided the relative DCH satellite intensities. R.P. participated in the identification of the shake contributions. L.I. performed the calculations of the Auger spectra. I.I. and L.I. drafted the manuscript. All authors contributed to the manuscript.

## APPENDIX A: CONTRIBUTIONS DUE TO SHAKE PROCESSES

In Fig. 7, we show complementary calculated Auger spectra for selected  $K^{-2}V^{-1}$  [Fig. 7(a)] and  $K^{-2}V^{-1}V'V''$  [Fig. 7(b)] configurations, i.e., double-core-hole configurations with an additional valence hole or with an additional valence hole and two electrons in virtual orbitals. In contrast to the results presented in the main text, for these calculations, only the equilibrium molecular geometry has been considered, and the resulting transitions have been convoluted with a Gaussian function with a full width at half maximum of 1.5 eV. For each configuration, the initial double-core- and valence-ionized or valence-excited state have been optimized in a multiple-configuration self-consistent-field calculation. The calculation procedure is otherwise the same as described in Sec. III. The results show that the Auger spectra of these additionally valence-ionized and valence-excited configurations have strong contributions in the region 530–540 eV. This points to the fact that the mismatch between the

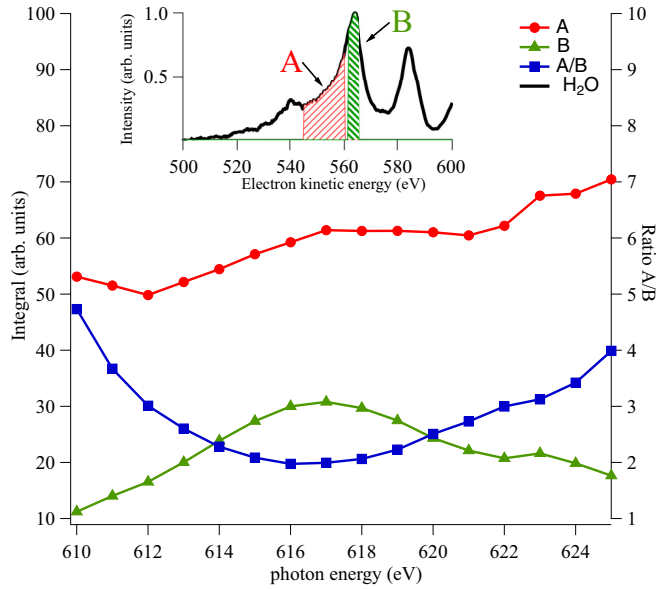


FIG. 8. Integrated Auger electron yield for the energy ranges 545–560 and 562–565 eV (indicated in the inset) as a function of photon energy. The blue line with squares indicates the ratio of the two energy ranges.

experimentally measured Auger spectra and the calculations in Figs. 2 and 3 can be attributed to these configurations.

The presence of  $K^{-2}V^{-1}$  configurations is plausible due to shake-off processes accompanying the core ionization, as well as direct valence ionization via three-photon absorption. At a photon energy of 617 eV, the presence of  $K^{-2}V^{-1}V'V''$  configurations is plausible via initial photoionization plus shake-up and subsequent core excitation. Moreover, for photon energies below the  $K^{-1} \rightarrow K^{-2}$  threshold,  $K^{-2}$  configurations can also be created via shake-off in the first photoionization step [27]. We stress that shake transitions in the context of core-shell photoabsorption amount to an overall contribution of 20% [46]. Considering that here two sequential photoabsorption steps are involved, it becomes very plausible that these processes yield considerable additional Auger signal.

A strong indication for the impact of shake-process-related electronic configurations on the DCH-Auger spectra can also be found in the experimental data, namely, by inspecting the Auger-electron spectra in the  $K^{-2}V$  region as a function of photon energy. The experimental data for this analysis were recorded with slightly different experimental parameters (see details in Ref. [27]), and because of the somewhat lower statistics, we consider Auger-electron spectra integrated over selected energy ranges. Figure 8 depicts the integrated signal strength for the dominant DCH-Auger peak (562–565 eV) and the gap region (545–560 eV). As expected, the dominant DCH-Auger peak decreases when the photon energy moves away from the  $K^{-1} \rightarrow K^{-2}4a_1$  transition energy of 617 eV.

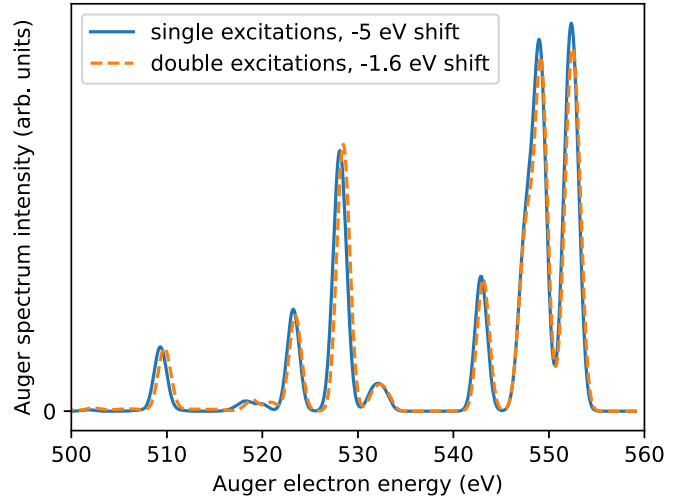


FIG. 9. Calculated DCH-Auger spectra (equilibrium geometry only). The solid line shows results obtained with the configurational truncation described in Sec. III. The dashed line shows results employing an extended configurational space (see text).

However, in contrast to this behavior, the Auger yield in the region of 545–560 eV steadily increases with photon energy, strongly indicating that it belongs to a background signal caused by different types of double-core-hole configurations. The trend that this background signal increases with photon energy matches our assessment that this signal involves shake transitions that become more and more available with larger photon energy. We thus assign the mismatch between calculated and experimentally observed spectra in Figs. 2 and 3 to the impact of such shake transitions.

## APPENDIX B: CONVERGENCE OF THE CALCULATIONS WITH RESPECT TO CONFIGURATIONAL SPACE

In the calculation of the Auger spectra, we truncated the configurational expansion to make the calculations feasible. This truncation leads to an unbalanced description of the initial and final electronic states. As a consequence, the Auger spectra had to be shifted by 5 eV in order to compare them with experimentally measured spectra. In Fig. 9, we show the results of our computation of the Auger spectra employing an extended configuration space. Specifically, initial and final electronic states are also described using configurations with excitation of two electrons into the virtual orbital space (two core holes, zero to two valence holes, and zero to two electrons in virtual orbitals for the initial states; one core hole, two to four valence holes, and zero to two electrons in virtual orbitals for the final states). Apart from the lower overall shift of 1.5 eV, the resulting spectra are almost identical, confirming that the shift is largely an artifact caused by the configurational truncation. We note that the remaining overall shift must partially be attributed to relativistic effects in the  $K$  shell [47], which are not considered in the calculation.

- [1] L. S. Cederbaum, F. Tarantelli, A. Sgamellotti, and J. Schirmer, On double vacancies in the core, *J. Chem. Phys.* **85**, 6513 (1986).
- [2] R. Santra, N. V. Kryzhevoi, and L. S. Cederbaum, X-ray two-photon photoelectron spectroscopy: A theoretical study of inner-shell spectra of the organic para-aminophenol molecule, *Phys. Rev. Lett.* **103**, 013002 (2009).
- [3] P. Salén, P. van der Meulen, H. T. Schmidt, R. D. Thomas, M. Larsson, R. Feifel, M. N. Piancastelli, L. Fang, B. Murphy, T. Osipov, N. Berrah, E. Kukk, K. Ueda, J. D. Bozek, C. Bostedt, S. Wada, R. Richter, V. Feyer, and K. C. Prince, Experimental verification of the chemical sensitivity of two-site double core-hole states formed by an x-ray free-electron laser, *Phys. Rev. Lett.* **108**, 153003 (2012).
- [4] M. Tashiro, M. Ehara, H. Fukuzawa, K. Ueda, C. Buth, N. V. Kryzhevoi, and L. S. Cederbaum, Molecular double core hole electron spectroscopy for chemical analysis, *J. Chem. Phys.* **132**, 184302 (2010).
- [5] N. Berrah *et al.*, Double-core-hole spectroscopy for chemical analysis with an intense x-ray femtosecond laser, *Proc. Natl. Acad. Sci. USA* **108**, 16912 (2011).
- [6] P. Lablanquie, T. P. Grozdanov, M. Žitnik, S. Carniato, P. Selles, L. Andric, J. Palaudoux, F. Penent, H. Iwayama, E. Shigemasa, Y. Hikosaka, K. Soejima, M. Nakano, I. H. Suzuki, and K. Ito, Evidence of single-photon two-site core double ionization of C<sub>2</sub>H<sub>2</sub> molecules, *Phys. Rev. Lett.* **107**, 193004 (2011).
- [7] D. Koulentianos *et al.*, Double-core-hole states in CH<sub>3</sub>CN: Pre-edge structures and chemical-shift contributions, *J. Chem. Phys.* **149**, 134313 (2018).
- [8] O. Takahashi, Theoretical double-core-hole spectroscopy of cytosine tautomers, *J. Electron Spectrosc. Relat. Phenom.* **223**, 72 (2018).
- [9] L. Inhester, G. Groenhof, and H. Grubmüller, Core hole screening and decay rates of double core ionized first row hydrides, *J. Chem. Phys.* **138**, 164304 (2013).
- [10] G. Goldsztejn, T. Marchenko, R. Püttner, L. Journal, R. Guillemin, S. Carniato, P. Selles, O. Travnikova, D. Céolin, A. F. Lago, R. Feifel, P. Lablanquie, M. N. Piancastelli, F. Penent, and M. Simon, Double-core-hole states in neon: Lifetime, post-collision interaction, and spectral assignment, *Phys. Rev. Lett.* **117**, 133001 (2016).
- [11] T. Marchenko, L. Inhester, G. Goldsztejn, O. Travnikova, L. Journal, R. Guillemin, I. Ismail, D. Koulentianos, D. Céolin, R. Püttner, M. N. Piancastelli, and M. Simon, Ultrafast nuclear dynamics in the doubly-core-ionized water molecule observed via Auger spectroscopy, *Phys. Rev. A* **98**, 063403 (2018).
- [12] M. Hoener *et al.*, Ultraintense x-ray induced ionization, dissociation, and frustrated absorption in molecular nitrogen, *Phys. Rev. Lett.* **104**, 253002 (2010).
- [13] L. Young *et al.*, Femtosecond electronic response of atoms to ultra-intense x-rays, *Nature (London)* **466**, 56 (2010).
- [14] S.-K. Son, R. Boll, and R. Santra, Breakdown of frustrated absorption in x-ray sequential multiphoton ionization, *Phys. Rev. Res.* **2**, 023053 (2020).
- [15] G. Charkap and C. R. Hebd, Experimental study of the double ionization of the K shell of <sup>55</sup>Mn in the disintegration of <sup>55</sup>Fe by K-capture, *Seances Acad. Sci.* **237**, 243 (1953).
- [16] J. P. Briand, P. Chevallier, M. Tavernier, and J. P. Rozet, Observation of *K* hypersatellites and *KL* satellites in the x-ray spectrum of doubly *K*-ionized gallium, *Phys. Rev. Lett.* **27**, 777 (1971).
- [17] P. Richard, W. Hodge, and C. F. Moore, Direct observation of *Kα* hypersatellites in heavy-ion collisions, *Phys. Rev. Lett.* **29**, 393 (1972).
- [18] J. P. Briand, A. Touati, M. Frilley, P. Chevallier, A. Johnson, J. P. Rozet, M. Tavernier, S. Shafroth, and M. O. Krause, The structure of *K<sub>α</sub>* hypersatellite spectra of Cu, Ni and Fe as a test of intermediate coupling, *J. Phys. B* **9**, 1055 (1976).
- [19] E. P. Kanter, R. W. Dunford, B. Krässig, and S. H. Southworth, Double *K*-vacancy production in molybdenum by x-ray photoionization, *Phys. Rev. Lett.* **83**, 508 (1999).
- [20] Y. Hikosaka, P. Lablanquie, F. Penent, T. Kaneyasu, E. Shigemasa, J. H. D. Eland, T. Aoto, and K. Ito, Double photoionization into double core-hole states in Xe, *Phys. Rev. Lett.* **98**, 183002 (2007).
- [21] J. H. D. Eland, M. Tashiro, P. Linusson, M. Ehara, K. Ueda, and R. Feifel, Double core hole creation and subsequent Auger decay in NH<sub>3</sub> and CH<sub>4</sub> molecules, *Phys. Rev. Lett.* **105**, 213005 (2010).
- [22] P. Lablanquie, F. Penent, J. Palaudoux, L. Andric, P. Selles, S. Carniato, K. Bučar, M. Žitnik, M. Huttula, J. H. D. Eland, E. Shigemasa, K. Soejima, Y. Hikosaka, I. H. Suzuki, M. Nakano, and K. Ito, Properties of hollow molecules probed by single-photon double ionization, *Phys. Rev. Lett.* **106**, 063003 (2011).
- [23] T. Marchenko, S. Carniato, G. Goldsztejn, O. Travnikova, L. Journal, R. Guillemin, I. Ismail, D. Koulentianos, J. Martins, D. Céolin, R. Püttner, M. N. Piancastelli, and M. Simon, Single and multiple excitations in double-core-hole states of free water molecules, *J. Phys. B* **53**, 224002 (2020).
- [24] S. Carniato, P. Selles, L. Andric, J. Palaudoux, F. Penent, M. Žitnik, K. Bučar, M. Nakano, Y. Hikosaka, K. Ito, and P. Lablanquie, Single photon simultaneous K-shell ionization and K-shell excitation. I. Theoretical model applied to the interpretation of experimental results on H<sub>2</sub>O, *J. Chem. Phys.* **142**, 014307 (2015).
- [25] T. Mazza *et al.*, Mapping resonance structures in transient core-ionized atoms, *Phys. Rev. X* **10**, 041056 (2020).
- [26] X. Li, L. Inhester, T. Osipov, R. Boll, R. Coffee, J. Cryan, A. Gatton, T. Gorkhover, G. Hartman, M. Ilchen, A. Knie, M.-F. Lin, M. P. Minitti, C. Weninger, T. J. A. Wolf, S.-K. Son, R. Santra, D. Rolles, A. Rudenko, and P. Walter, Electron-ion coincidence measurements of molecular dynamics with intense x-ray pulses, *Sci. Rep.* **11**, 505 (2021).
- [27] I. Ismail *et al.*, Alternative pathway to double-core-hole states, *Phys. Rev. Lett.* **131**, 253201 (2023).
- [28] O. Travnikova, N. Sisourat, T. Marchenko, G. Goldsztejn, R. Guillemin, L. Journal, D. Céolin, I. Ismail, A. F. Lago, R. Püttner, M. N. Piancastelli, and M. Simon, Subfemtosecond control of molecular fragmentation by hard x-ray photons, *Phys. Rev. Lett.* **118**, 213001 (2017).
- [29] T. Marchenko, G. Goldsztejn, K. Jänkälä, O. Travnikova, L. Journal, R. Guillemin, N. Sisourat, D. Céolin, M. Žitnik, M. Kavčič, K. Bučar, A. Mihelič, B. Cunha de Miranda, I. Ismail, A. F. Lago, F. Gel'mukhanov, R. Püttner, M. N. Piancastelli, and M. Simon, Potential energy surface reconstruction and lifetime determination of molecular double-core-hole states in the hard x-ray regime, *Phys. Rev. Lett.* **119**, 133001 (2017).



- [30] L. Inhester, C. F. Burmeister, G. Groenhof, and H. Grubmüller, Auger spectrum of a water molecule after single and double core ionization, *J. Chem. Phys.* **136**, 144304 (2012).
- [31] T. Tschentscher, C. Bressler, J. Grünert, A. Madsen, A. P. Mancuso, M. Meyer, A. Scherz, H. Sinn, and U. Zastra, Photon beam transport and scientific instruments at the European XFEL, *Appl. Sci.* **7**, 592 (2017).
- [32] T. Mazza *et al.*, The beam transport system for the Small Quantum Systems instrument at the European XFEL: Optical layout and first commissioning results, *J. Synchrotron Radiat.* **30**, 457 (2023).
- [33] W. Decking *et al.*, A MHz-repetition-rate hard x-ray free-electron laser driven by a superconducting linear accelerator, *Nat. Photon.* **14**, 391 (2020).
- [34] A. De Fanis *et al.*, High-resolution electron time-of-flight spectrometers for angle-resolved measurements at the SQS instrument at the European XFEL, *J. Synchrotron Radiat.* **29**, 755 (2022).
- [35] Y. Hao, L. Inhester, K. Hanasaki, S.-K. Son, and R. Santra, Efficient electronic structure calculation for molecular ionization dynamics at high x-ray intensity, *Struct. Dyn.* **2**, 041707 (2015).
- [36] L. Inhester, K. Hanasaki, Y. Hao, S.-K. Son, and R. Santra, X-ray multiphoton ionization dynamics of a water molecule irradiated by an x-ray free-electron laser pulse, *Phys. Rev. A* **94**, 023422 (2016).
- [37] P. S. Bagus, Self-consistent-field wave functions for hole states of some Ne-like and Ar-like ions, *Phys. Rev.* **139**, A619 (1965).
- [38] A. T. B. Gilbert, N. A. Besley, and P. M. W. Gill, Self-consistent field calculations of excited states using the maximum overlap method (MOM), *J. Phys. Chem. A* **112**, 13164 (2008).
- [39] T. H. Dunning, Jr., Gaussian basis sets for use in correlated molecular calculations. I. The atoms boron through neon and hydrogen, *J. Chem. Phys.* **90**, 1007 (1989).
- [40] R. A. Kendall, T. H. Dunning, Jr., and R. J. Harrison, Electron affinities of the first-row atoms revisited. Systematic basis sets and wave functions, *J. Chem. Phys.* **96**, 6796 (1992).
- [41] H. Siegbahn, L. Asplund, and P. Kelfve, The Auger electron spectrum of water vapour, *Chem. Phys. Lett.* **35**, 330 (1975).
- [42] Z. Jurek, S.-K. Son, B. Ziaja, and R. Santra, *XMDYN* and *XATOM*: Versatile simulation tools for quantitative modeling of x-ray free-electron laser induced dynamics of matter, *J. Appl. Crystallogr.* **49**, 1048 (2016).
- [43] A. Sankari, C. Stråhlman, R. Sankari, L. Partanen, J. Laksman, J. A. Kettunen, I. F. Galván, R. Lindh, P.-Å. Malmqvist, and S. L. Sorensen, Non-radiative decay and fragmentation in water molecules after  $1a_1^{-1}4a_1$  excitation and core ionization studied by electron-energy-resolved electron-ion coincidence spectroscopy, *J. Chem. Phys.* **152**, 074302 (2020).
- [44] F. Trinter, L. Inhester, R. Püttner, S. Malerz, S. Thürmer, T. Marchenko, M. N. Piancastelli, M. Simon, B. Winter, and U. Hergenhan, Radiationless decay spectrum of O 1s double core holes in liquid water, *J. Chem. Phys.* **160**, 194503 (2024).
- [45] European XFEL, Proposal No. 002620, <https://doi.org/10.22003/XFEL.EU-DATA-002620-00>.
- [46] A. G. Kochur and V. A. Popov, Probabilities of multiple shake processes in sudden approximation, *J. Phys. B* **39**, 3335 (2006).
- [47] J. Niskanen, P. Norman, H. Aksela, and H. Ågren, Relativistic contributions to single and double core electron ionization energies of noble gases, *J. Chem. Phys.* **135**, 054310 (2011).